Electronic Supplementary Material (ESI) for Environmental Science: Nano.

Supplementary Information

Generation of Environmentally Persistent Free Radicals on Faceted TiO_2 in an Ambient Environment: Roles of Crystalline Surface Structures

Di Lang [a], Feng Jiang [a], Peng Yi [a], Xu Gao [a], Yi Liu [a], Hao Li [a], Quan Chen [a], Bo Pan [a] *, and Baoshan Xing [b]

[a] Yunnan Provincial Key Lab of Soil Carbon Sequestration and Pollution Control, Faculty of Environmental Science & Engineering, Kunming University of Science & Technology, Kunming, 650500, China

[b] Stockbridge School of Agriculture, University of Massachusetts, Amherst, MA 01003, United States

* Corresponding author: B.P., phone: 86-871-65170906, Email: panbocai@gmail.com

Contents:

Number of pages: 22

Figures: 11

Tables: 2

References: 5

Section 1. Chemicals

Catechol (99%; Aladdin, China); Hydrofluoric acid (48%; Aladdin, China); TiO_2 nanoparticles (P25, 99.5%; Sigma-Adlrich, U.S.A.); Ethanol (HPLC; Aladdin, China); NaOH (99%; Sinopharm Chemical Reagent, China); Anatase TiO_2 (97%, Sinopharm Chemical Reagent, China); Butyl titanate (IV) (48%, Aladdin, China); Potassium hydroxide (99%, Sinopharm Chemical Reagent, China); Acetic acid (99%, Sinopharm Chemical Reagent, China);

Section 2. Synthesis of {001}, {010}, and {101}-TiO_2 nanoparticles

{001}-TiO_2 was synthesized by hydrothermal method.[1] 3 mL of hydrofluoric acid and 25 mL butyl titanate (IV) were mixed in a Teflon-lined stainless steel autoclave and heated at 200 °C for 24 h. The white product was washed alternately with ultrapure water and ethanol until it was nearly neutral. The product was immersed in NaOH (0.1 $mol\cdot L^{-1}$, 100 mL) solution overnight, and then the powder was repeatedly washed alternately with ultra-pure water and ethanol five times. The white precipitate was centrifuged and dried at 120 °C to obtain {001}-TiO_2 nanoparticles.

{010}-TiO_2 was synthesized by a two-step hydrothermal method.[2] The first step, 978 mg anatase TiO_2 powder was mixed with NaOH (10 $mol\cdot L^{-1}$) solution. The mixture was transferred to a stainless steel autoclave with Teflon lining and heated at 180 °C for 24 h. The resulting $Na_{1-x}H_xTiO_3$ nanoparticles were separated from the suspension by high-speed centrifugation, washed with deionized water to remove all excess NaOH and dried at 80 °C. The second step, the dried powder was ultrasonically mixed with hydrochloric acid solution and then stirred with a magnetic stirrer for 20 min to form $HTiO_3$ nanotubes. The white powder was collected by high-speed centrifugation and washed several times with deionized water until all hydrochloric acid was removed and dried at 80 °C. 200 mg white powder was evenly mixed with 100 mL ultrapure water and transferred to stainless steel autoclave, which was heated at 170 °C for 16 h, so that the $HTiO_3$ nanotubes could be converted into TiO_2. The white precipitate was collected by high-speed centrifugation, washed with deionized water several times, and dried at 120 °C to get the final product.

{101}-TiO_2 was synthesized by a two-step hydrothermal method.[3] The first step, 1 g TiO_2 nanoparticles (P25) were evenly mixed with 40 mL potassium hydroxide (17 $mol \cdot L^{-1}$) solution and then transferred to a stainless steel autoclave with Teflon lining and heated at 110 °C for 20 h. The white precipitate was washed with deionized water and acetic acid aqueous solution to neutral and dried at 80 °C to obtain TiO_2 nanoparticles. The second step, the prepared 100 mg TiO_2 nanoparticles were evenly mixed with 30 mL deionized water and transferred to a Teflon-lined autoclave, heated at 170 °C for 24 h. The white precipitate was isolated by high-speed centrifugation, and dried at 120 °C to obtain the final product.

Section 3. The load method of CT

CT was loaded on as-prepared TiO_2 nanoparticles with three kinds of loading methods in dark: (1) TiO_2 nanoparticles were soaked in a CT solution and then dried by lyophilization. 80 mg TiO_2 powder and 1 mL Catechol (CT) aqueous solution (300 mg/L) were mixed in 8 mL brown glass bottles, placed in an oscillator for 5 h at 25 °C, frozen for 2 h, and freeze-dried for 12 h; (2) TiO_2 nanoparticles were soaked in a CT methanol solution and then dried by a nitrogen blowing concentrator. 80 mg TiO_2 powder and 1 mL CT (300 mg/L) methanol solution were mixed in an 8 mL brown glass bottle, placed in an oscillator for 5 h, and then the methanol was blow dry with nitrogen. (3) CT was loaded on TiO_2 nanoparticles by chemical vapor deposition. 10 mg TiO_2 powder and 10 mg pure CT were placed on both sides of the watch glass, and closed the caps. Then the watch glass was placed in an oven and heated at 60 °C for 12 h.

Section 4. Characterization

X-ray diffraction (XRD) of as-prepared samples were recorded on an X-ray diffractometer (D/Max-2200, Rigaku, Japan) using Cu Kα irradiation (k=0.154054 nm), operating at 40 mA and 40 kV. A Tecnai G2 F30 S-TWIN (Thermo Fisher Scientific, U.S.A.) TEM conducted transmission electron microscopy (TEM) analyses at an acceleration voltage of 120 kV. The specific surface area (SSA) and pore size distribution of particles were determined using the BET method (ASAP 2020, Micromeritics, U.S.A.). X-ray photoelectron spectroscopy (XPS) of samples were recorded on an ESCALAB 250XI spectrometer (Thermo Fisher Scientific, U.S.A.) using an Al Kα X-ray source. The UV-vis diffuse reflectance spectra of samples were detected on a UV/vis spectrophotometer (TU-1901, PERSEE, China). The surface functional groups evolution of {010}-TiO_2-CT under light was characterized by Fourier infrared spectra (FT-IR, Nicolet-Is10, Thermo Scientific, USA). The electrochemical impedance spectroscopy (EIS) of different faceted TiO_2 was recorded by an electrochemical workstation (CHI620E, Shanghaichenhua, Shanghai, China) according to the previously reported method.[4] The test parameters apply an AC voltage amplitude of 100 mV at 0.55 V within a frequency range of 0.1-10^5 Hz. Photoluminescence (PL) spectra of faceted TiO_2 particles were recorded on a PL instrument (FLS980, Edinburgh Instruments, Britain) with an excitation wavelength of 325 nm at room temperature.

Figures

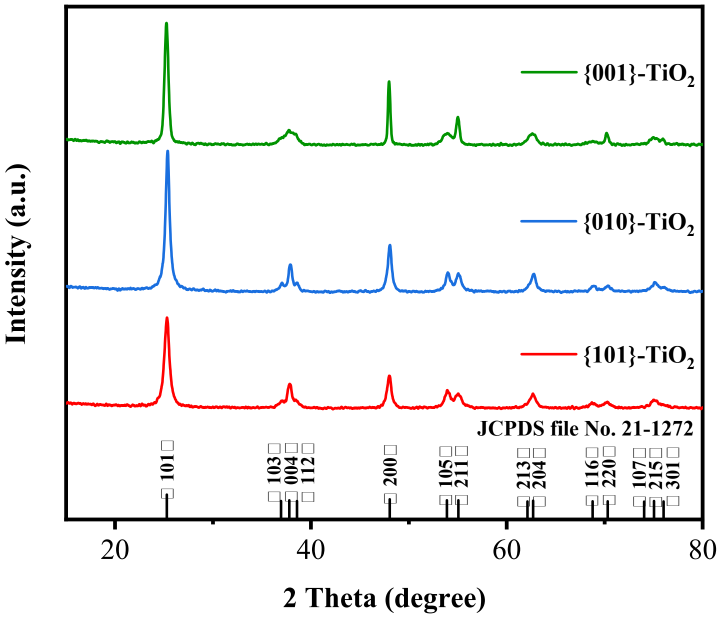

Fig. S1. XRD patterns of the as-prepared TiO$_2$ samples.

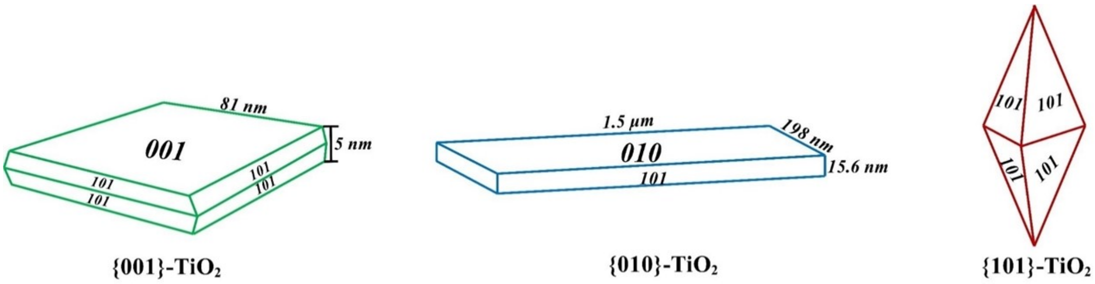

Fig. S2. Schematic structure of the as-prepared TiO$_2$ samples.

The {001}-TiO$_2$ samples have a plate-like morphology, and their average side length and thickness are measured to be 81 nm and 5 nm, respectively (Fig. 1(A)). Based on the schematic structure, we can calculate the percentage of {001} facet on {001}-TiO$_2$ according to a previously reported formula as follows,[1] where θ, a and h represent the angle between {001} facet and {101} facet of anatase (68.3°), and the length and thickness of {001}-TiO$_2$, respectively.[5]

$$S_{(001)} = \cos(\theta)/(\cos(\theta) + \left(\frac{a}{a + \frac{h}{\tan(\theta)}}\right)^{-2} - 1)$$

$$S_{(001)} = \frac{\cos(68.3^{\circ})}{\cos(68.3^{\circ}) + \left(\frac{81}{81 + \frac{5}{\tan(68.3^{\circ})}}\right)^{-2} - 1} \approx 88.1\%$$

{010}-TiO$_2$ particles are composed of many nanobelts, which are measured to have an average length of 1.5 μm, a width of 198 nm, and a thickness of 16.5 nm (Fig. 1(B)). Based on the above schematic structure and the equation below,[1] we can deduce the exposure percentage of the {010} facet on {010}-TiO$_2$. The a, b, and c represent the length, width, and thickness, respectively.

$$S_{(010)} = \frac{2ab}{2(ab + ac + bc)}$$

$$S_{(010)} = \frac{2 \times 1500 \times 198}{2(1500 \times 198 + 1500 \times 16.5 + 198 \times 16.5)} = 91.4\%$$

The {101}-TiO$_2$ has an octahedral geometry according to the schematic structure in Fig. S2, and all eight facets on {101}-TiO$_2$ are the {101} facet. As shown in Fig. 1(C), the prepared sample shows a rhombic structure. We can infer that the predominantly exposed facet accounted for over 90% of the total crystal area combined with the schematic structure.

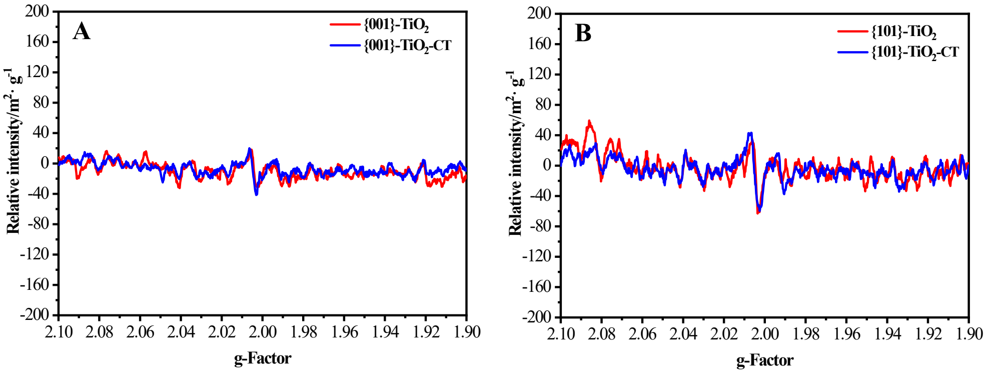

Fig. S3. EPR signals of {001} and {010}-TiO$_2$ before and after CT loading.

(Standardization by specific surface area)

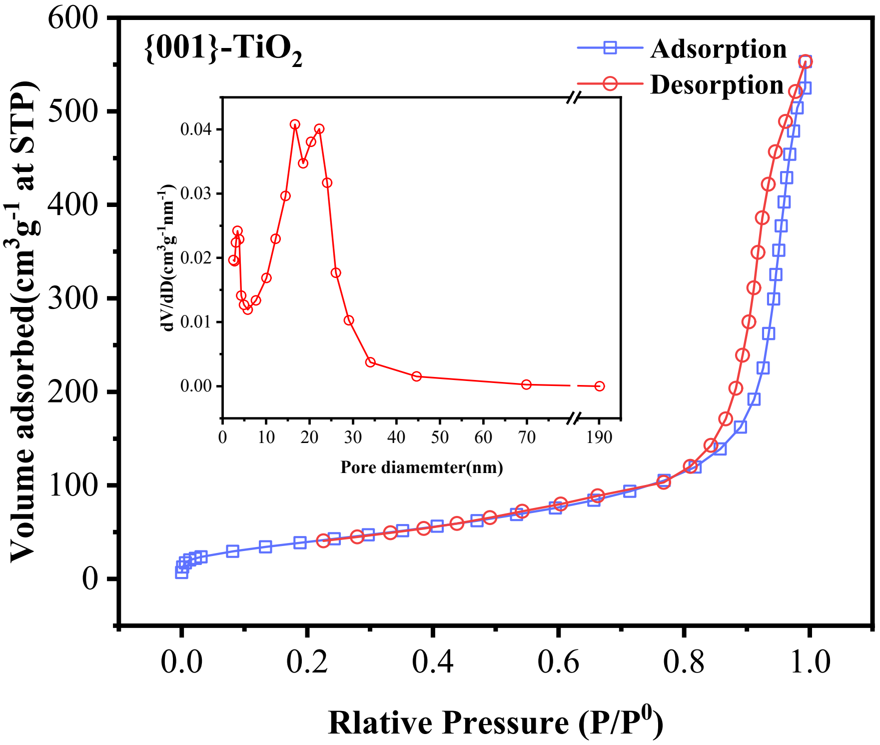
{001}-TiO$_2$
Adsorption
Desorption
Volume adsorbed(cm^{3}g^{-1} at STP)
600
500
400
300
200
100
0
0.0
0.2
0.4
0.6
0.8
1.0
Rlative Pressure (P/P^0)
dV/dD(cm^{3}g^{-1}nm^{-1})
0.04
0.03
0.02
0.01
0.00
0
10
20
30
40
50
60
70
190
Pore diamemter(nm)

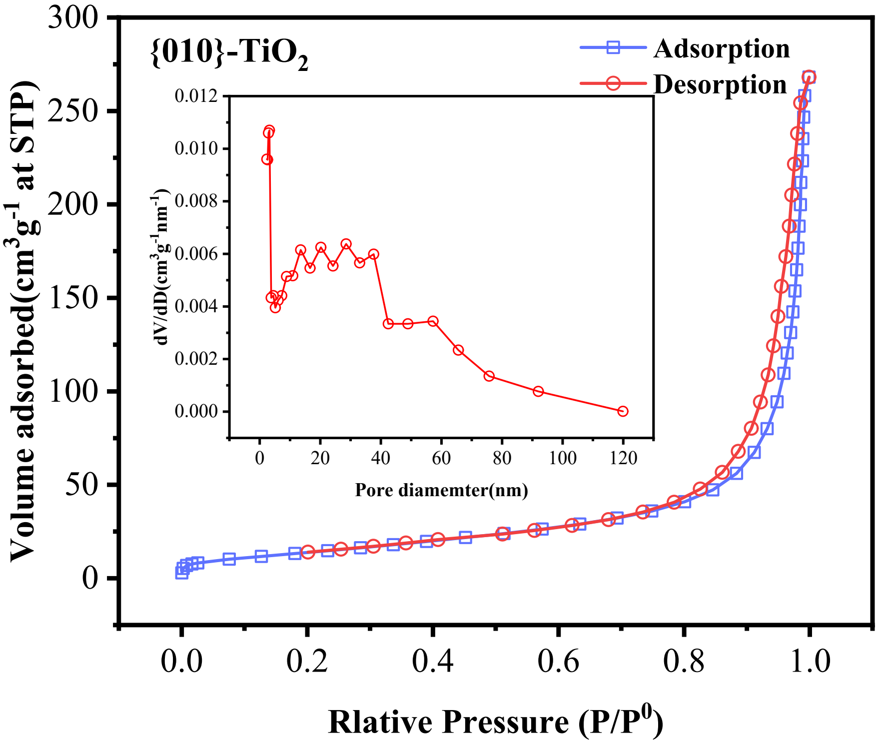
{010}-TiO$_2$
Adsorption
Desorption
Volume adsorbed(cm^{3}g^{-1} at STP)
300
250
200
150
100
50
0
0.0
0.2
0.4
0.6
0.8
1.0
Rlative Pressure (P/P^0)
dV/dD(cm^{3}g^{-1}nm^{-1})
0.012
0.010
0.008
0.006
0.004
0.002
0.000
0
20
40
60
80
100
120
Pore diamemter(nm)

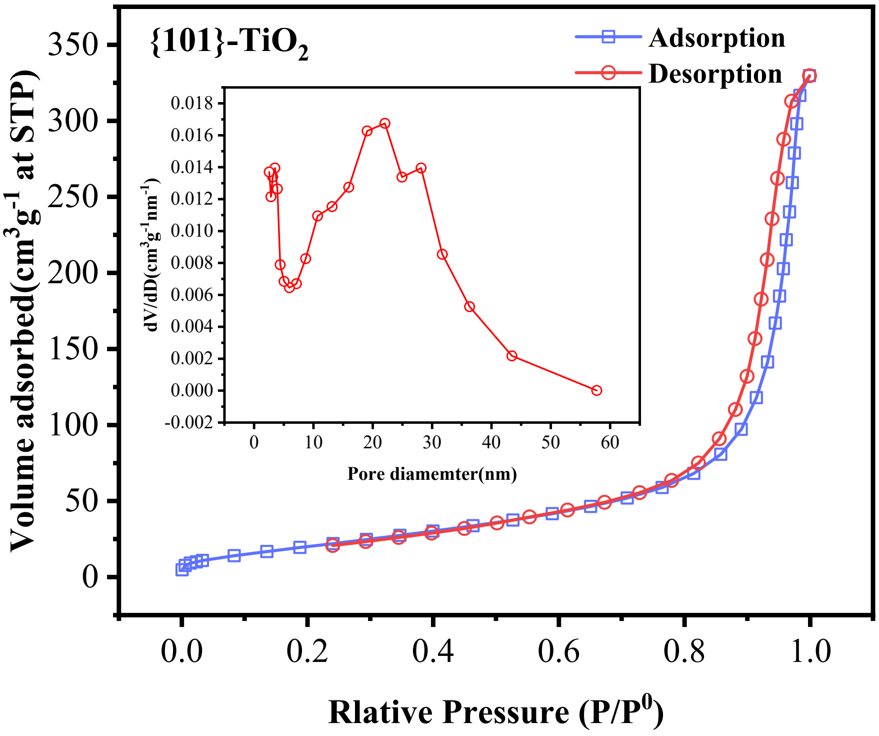

Fig. S4. Nitrogen adsorption−desorption isotherms and pore size distributions of {001}-TiO_2, {010}-TiO_2 and {101}-TiO_2.

Nitrogen adsorption-desorption (Fig. S4) was used to investigate the surface properties of {001}-TiO_2, {010}-TiO_2 and {101}-TiO_2. Surface area, pore diameter, and pore volume data are shown in Table S1. The nitrogen adsorption-desorption isotherms of the three faceted TiO_2 samples are all showed obvious hysteresis loops in the range of relative pressure from 0.8 to 1.0 and correspond to the type IV isotherms. The pore diameter distribution showed that these three nanoparticles exhibited mesoporous structures with average pore diameters of 22–31 nm.

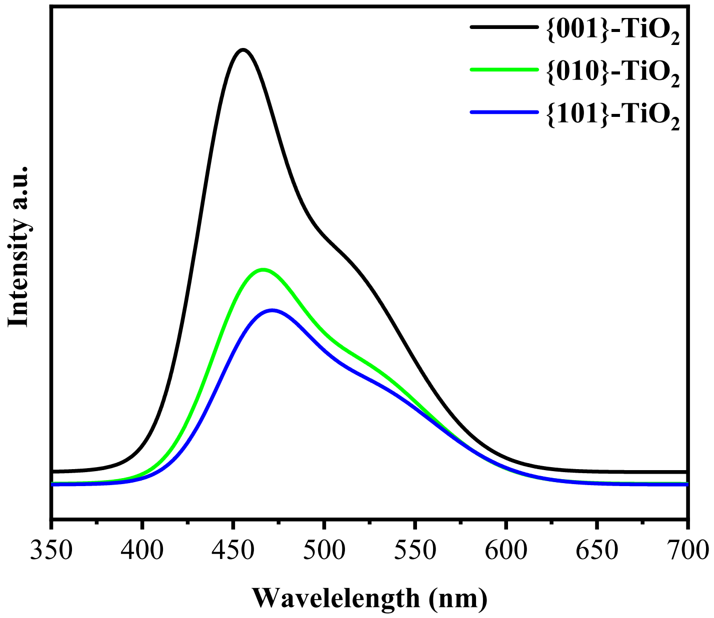

Fig. S5. PL spectrum of {001}-TiO_2, {010}-TiO_2 and {101}-TiO_2.

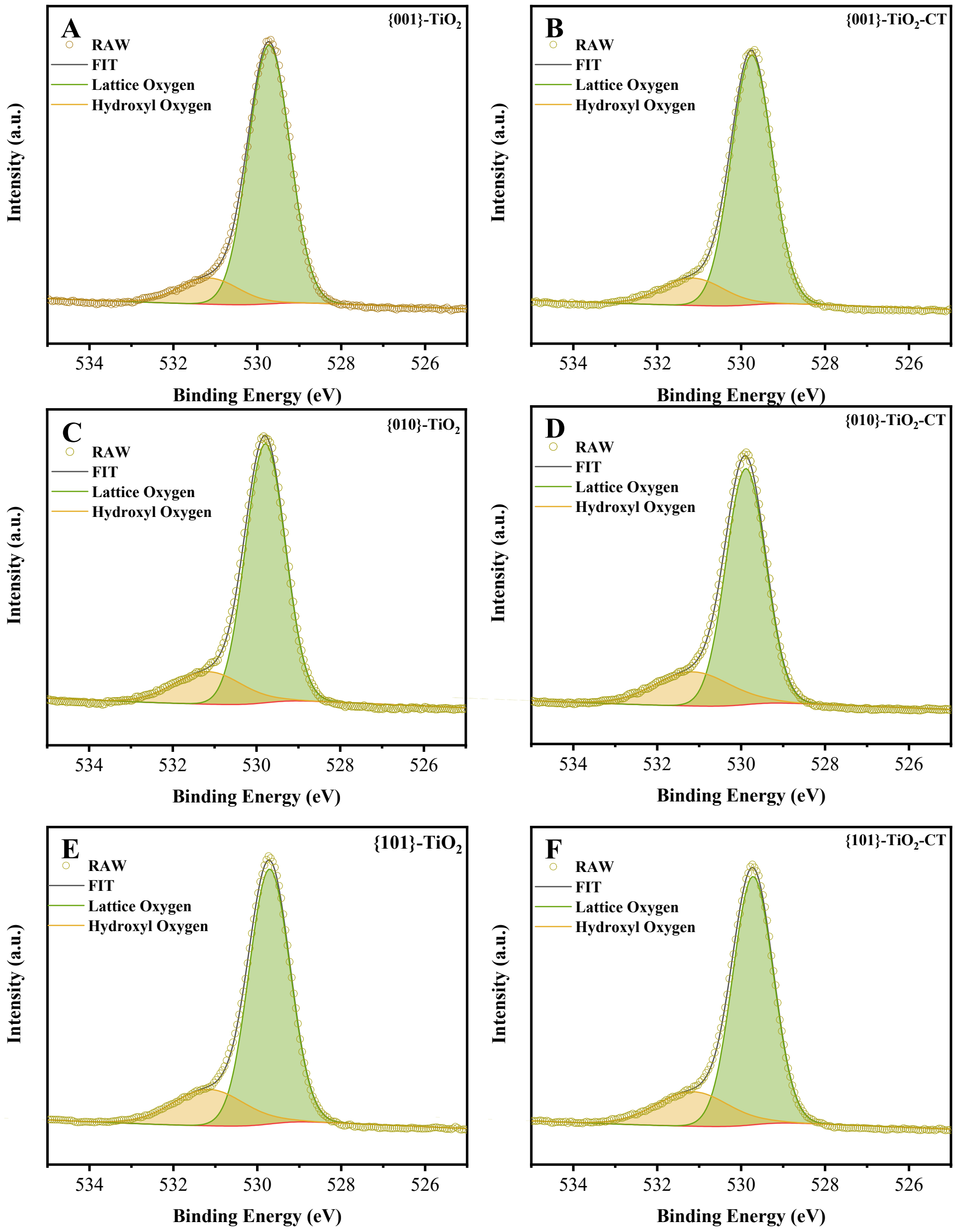

Fig. S6. The high-resolution O 1s spectrum of three faceted TiO_2 before and after CT adsorption.

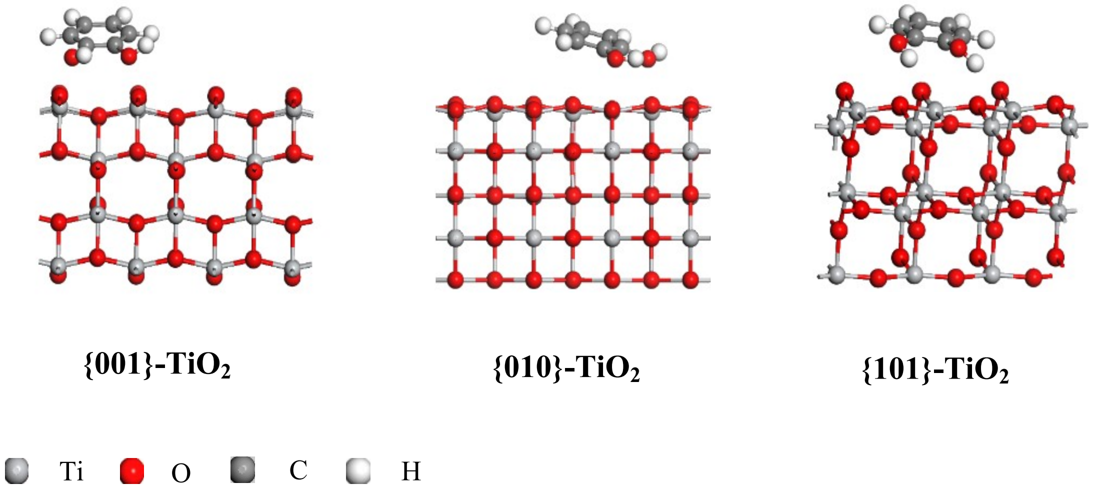

{001}-TiO$_2$ **{010}-TiO$_2$** **{101}-TiO$_2$**

Fig. S7. Adsorption equilibrium configuration images of CT adsorption on {001}-TiO$_2$, {010}-TiO$_2$, and {101}-TiO$_2$ particles. The {001} facet was composed of 98 O atoms and 49 Ti atoms, the {010} facet was composed of 70 O atoms and 35 Ti atoms, and the {101} facet was composed of 90 O atoms and 48 Ti atoms.

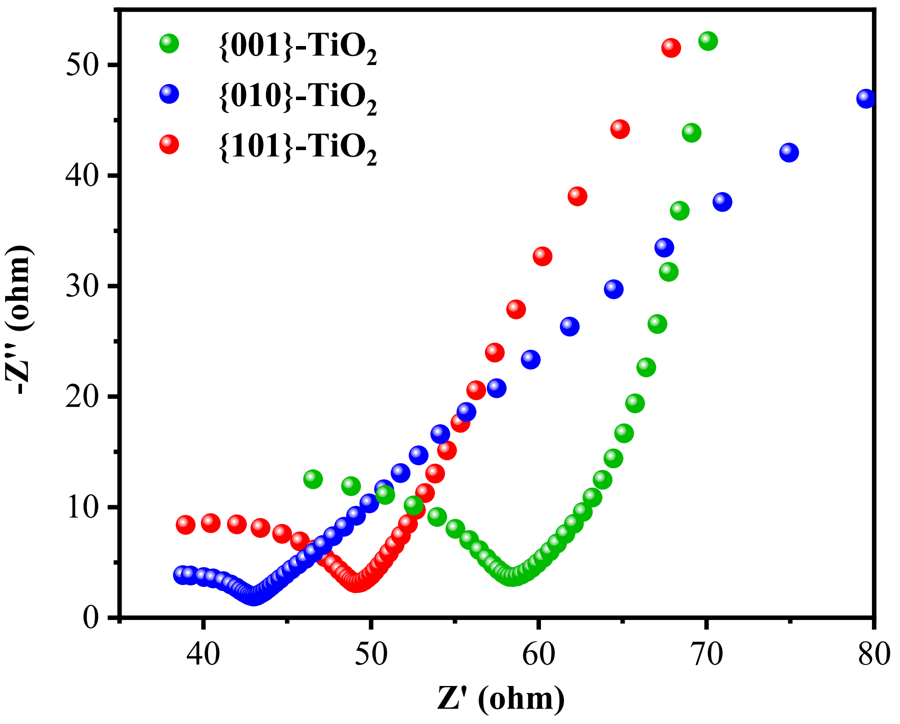

Fig. S8. Electrochemical impedance of different faceted TiO_2 in the dark.

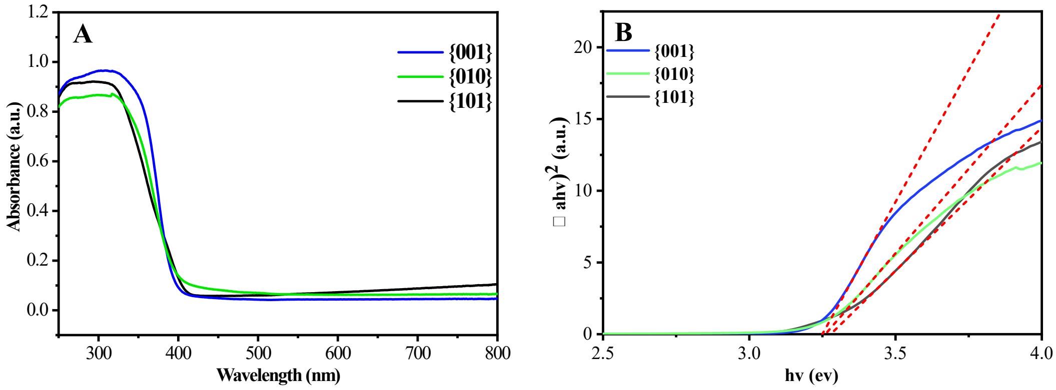

Fig. S9. UV-vis diffuse reflectance spectra of three faceted TiO_2 particles before (A) and after (C) CT adsorption, and Plots of the $(\alpha h\nu)^2$ *vs.* photon energy ($h\nu$) of the prepared faceted TiO_2 samples.

The bandgaps of these faceted TiO_2 particles were determined from diffuse reflectance spectroscopy (Fig. S9-A). The responses of {001}-TiO_2, {010}-TiO_2 and {101}-TiO_2 samples to UV light were basically the same, and the maximum absorption peaks all appeared at approximately 310 nm. The bandgaps of {001}-TiO_2, {010}-TiO_2 and {101}-TiO_2 were 3.25 eV, 3.26 eV and 3.28 eV, respectively; these were calculated by an extrapolation method, as presented in Fig. S9-B. The band gaps of the three faceted samples were close, which further proved that they have the same crystal phase structure. The slight difference in the band gap was mainly due to a subtle change in the Fermi surface caused by atomic structural distortion of the highly exposed crystal plane.

Catechol

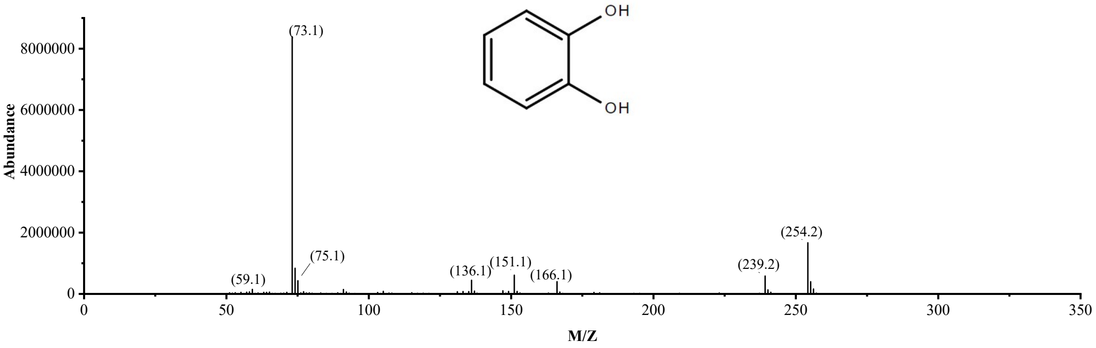

pyrogallol

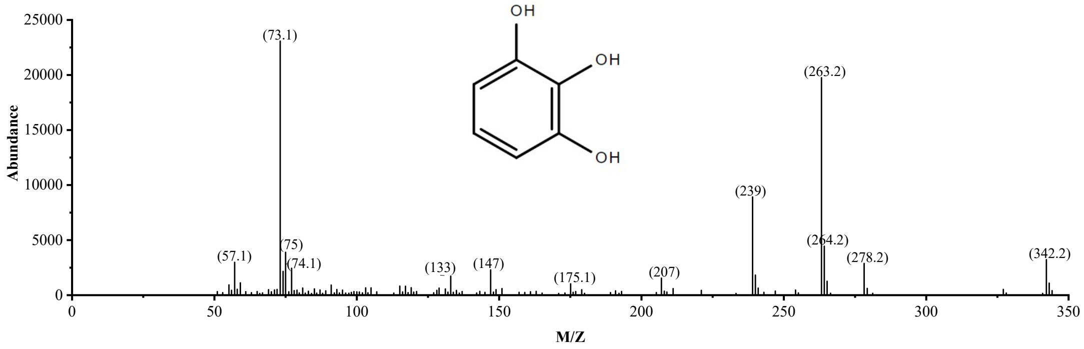

1,2,4-Benzenetriol

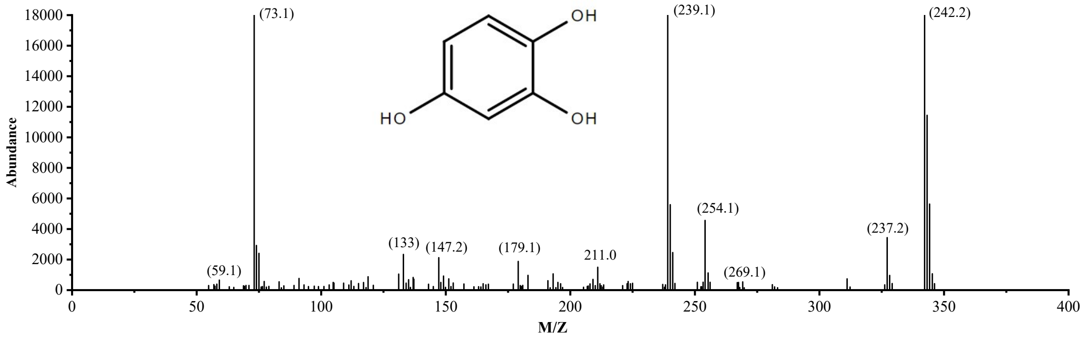

Salicylic acid

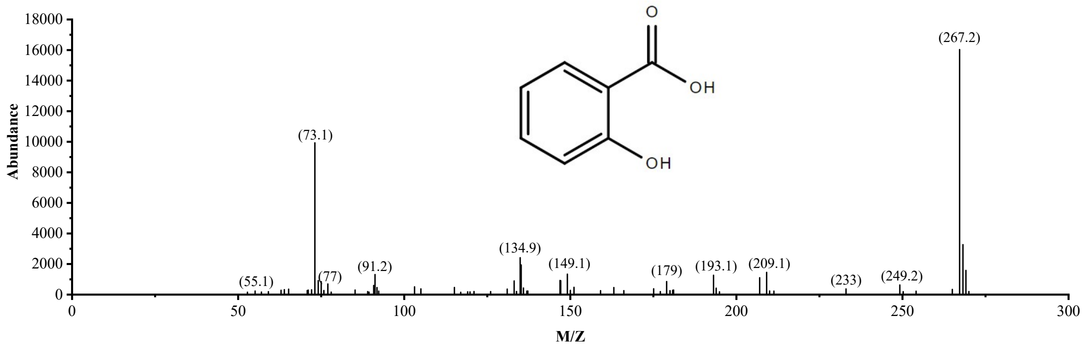

Benzoic Acid

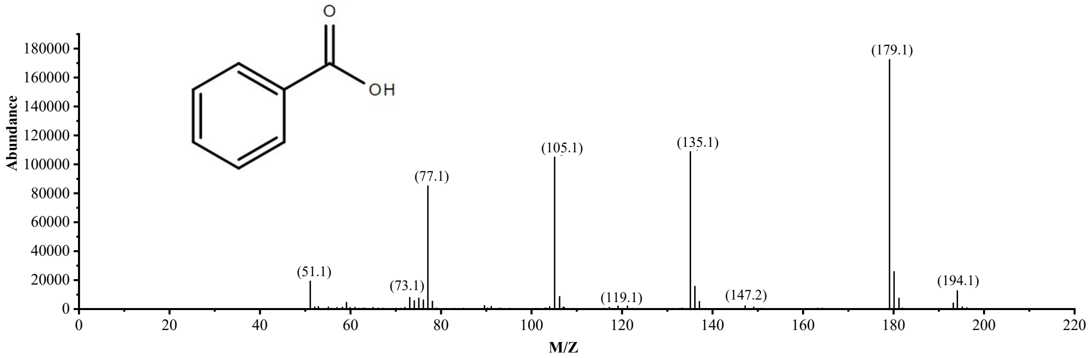

Ethylene glycol

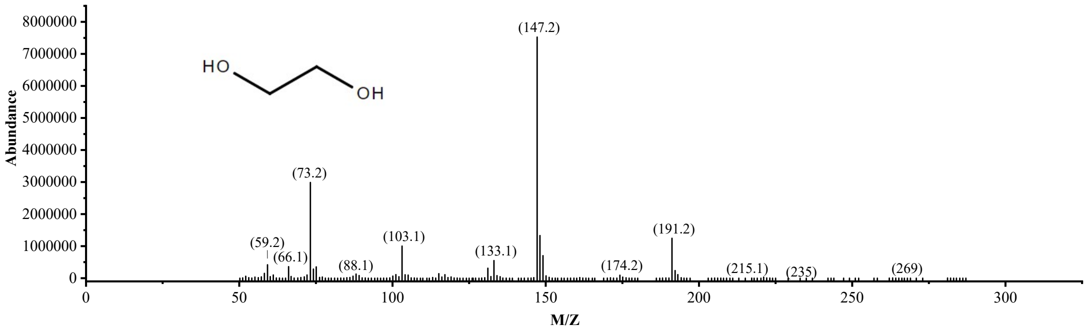

Hydracrylic acid

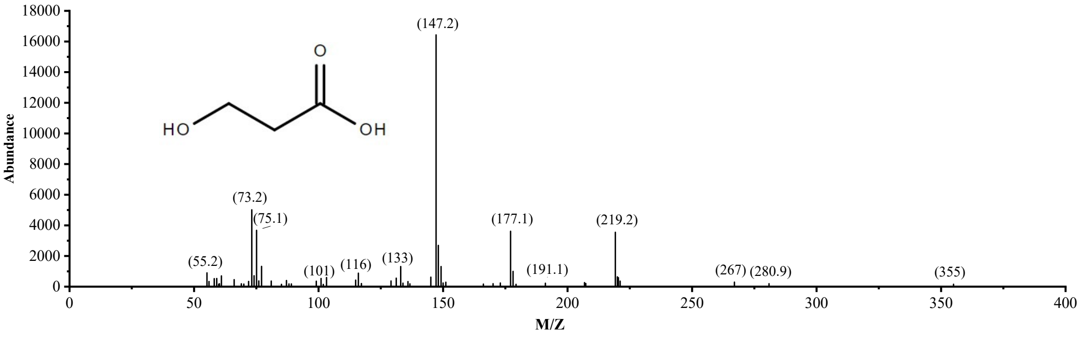

Palmitic Acid

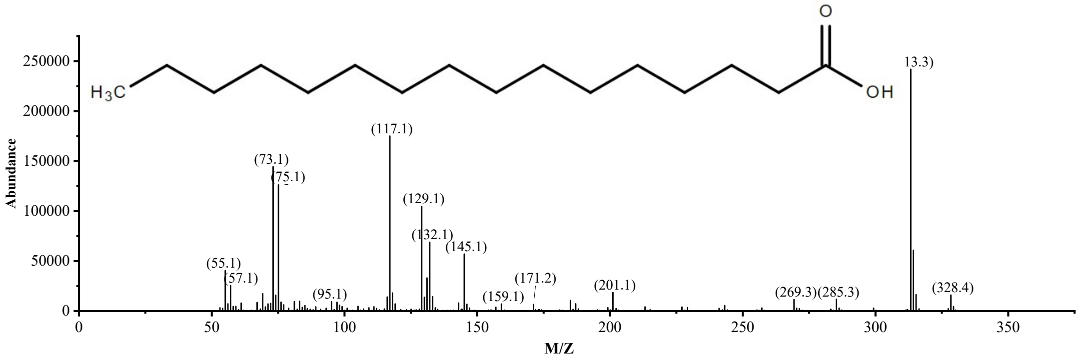

Nonanoic acid

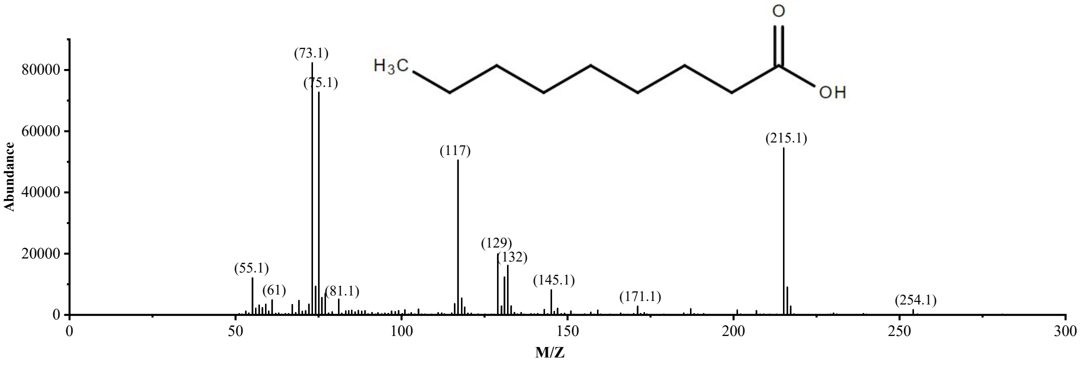

9,18-Dihydroxyoctadecanoic acid

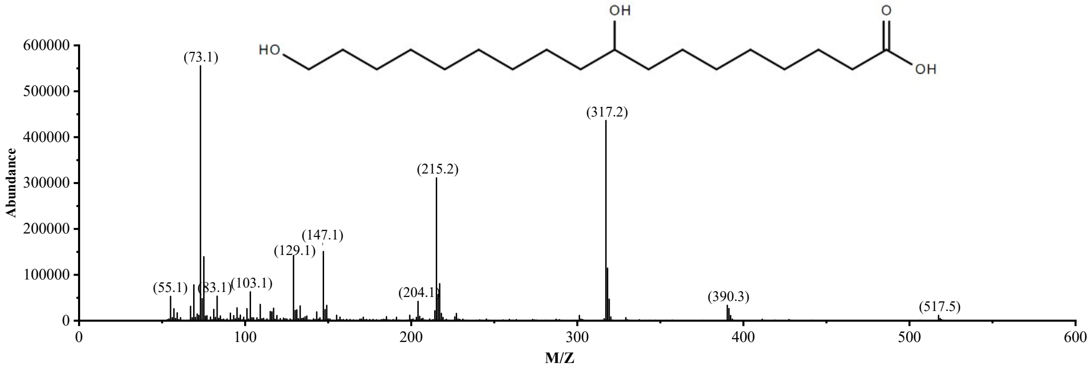

Fig. S10. Mass spectrum of degradation products of CT on {010}-TiO_2 after UV irradiation for 2 hours.

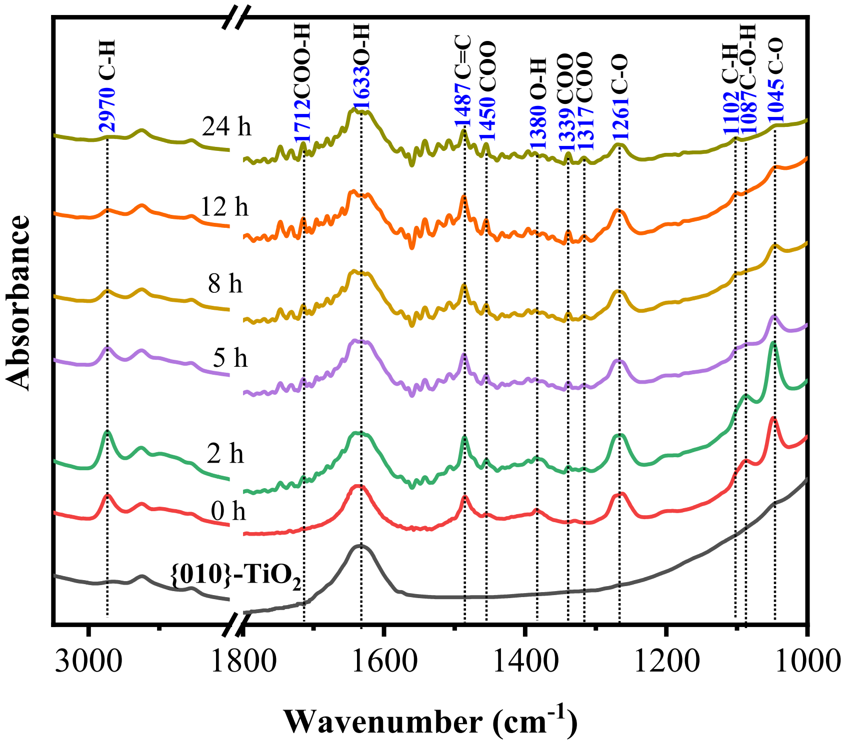

Fig. S11. Infrared spectrum of {001}-TiO$_2$ in the photoreaction process.

Tables

Table S1. BET Data of the Prepared Faceted TiO_2

Sample	Specific surface area S_{BET} (m^2/g)	Pore diameter ds (nm)	Pore volume pv (cm^3/g)
{001}- TiO_2	153.523	22.293	0.856
{010}- TiO_2	54.199	30.272	0.415
{101}- TiO_2	85.208	23.939	0.510

Table S2. The proportions of lattice oxygen and hydroxyl in O1s spectrum for all samples

Sample	Lattice Oxygen	Hydroxyl Oxygen
{001}-TiO_2	87.27%	12.73%
{001}-TiO_2-CT	85.60%	14.40%
{010}-TiO_2	82.31%	17.69%
{010}-TiO_2-CT	78.38%	21.62%
{101}-TiO_2	79.82%	20.18%
{101}-TiO_2-CT	79.92%	20.08%

Reference

1. C. Li, C. Koenigsmann, W. Ding, B. Rudshteyn, K. R. Yang, K. P. Regan, S. J. Konezny, V. S. Batista, G. W. Brudvig, C. A. Schmuttenmaer and J.-H. Kim, Facet-dependent photoelectrochemical performance of TiO_2 nanostructures: An experimental and computational study, *J. Am. Chem. Soc.*, 2015, **137**, 1520-1529.
2. Y. Mao and S. Wong, Size- and shape-dependent transformation of nanosized titanate into analogous anatase titania nanostructures, *J. Am. Chem. Soc.*, 2006, **128**, 8217-8226.
3. F. Amano, T. Yasumoto, O. O. P. Mahaney, S. Uchida, T. Shibayama, Y. Terada and B. Ohtani, Highly active titania photocatalyst particles of controlled crystal phase, size, and polyhedral shapes, *Top Catal.*, 2010, **53**, 455-461.
4. D. Lang, F. Y. Cheng and Q. J. Xiang, Enhancement of photocatalytic H-2 production activity of CdS nanorods by cobalt-based cocatalyst modification, *Catal. Sci. Technol.*, 2016, **6**, 6207-6216.
5. H. G. Yang, G. Liu, S. Z. Qiao, C. H. Sun, Y. G. Jin, S. C. Smith, J. Zou, H. M. Cheng and G. Q. Lu, Solvothermal synthesis and photoreactivity of anatase TiO_2 nanosheets with dominant {001} facets, *J. Am. Chem. Soc.*, 2009, **131**, 4078-4083.